UNIVERSITY OF CALGARY

**University of Calgary**

**PRISM: University of Calgary's Digital Repository**

Schulich School of Engineering | Schulich School of Engineering Research & Publications

2019-01

# High-Performance, Room Temperature Hydrogen Sensing With a Cu-BTC/Polyaniline Nanocomposite Film on a Quartz Crystal Microbalance

Abuzalat, Osama; Wong, Danny; Park, Simon S.; Kim, Seonghwan

http://hdl.handle.net/1880/111761
journal article

Unless otherwise indicated, this material is protected by copyright and has been made available with authorization from the copyright owner. You may use this material in any way that is permitted by the Copyright Act or through licensing that has been assigned to the document. For uses that are not allowable under copyright legislation or licensing, you are required to seek permission.

*Downloaded from PRISM: https://prism.ucalgary.ca*

# High-Performance, Room Temperature Hydrogen Sensing with a Cu-BTC/Polyaniline Nanocomposite Film on a Quartz Crystal Microbalance

Osama Abuzalat†, Danny Wong†, Simon S. Park, Seonghwan Kim*

*Department of Mechanical and Manufacturing Engineering, University of Calgary, Calgary, Alberta*

*T2N 1N4, Canada*

***Abstract*— In this article, we demonstrate a high-performance hydrogen sensor under ambient conditions by growing a Cu-BTC/polyaniline (PANI) nanocomposite film on a quartz crystal microbalance (QCM) using intense pulsed light. The QCM was first sputter coated with a 200 nm thin layer of copper. The copper layer was then oxidized by sodium hydroxide and ammonium persulfate. A solution containing the organic ligand (BTC) and PANI was then dropped and dried on the copper hydroxide surface of a QCM with intense pulsed light which resulted in Cu-BTC/PANI nanocomposite film on a QCM. The gas sensing performance of the Cu-BTC film and Cu-BTC/PANI composite film was compared under ambient conditions. It was found selectivity and sensitivity of the Cu-BTC/PANI nanocomposite film to hydrogen were significantly improved. In addition, a fast response time (from 2 to 5 seconds), operation at room temperature even in the presence of high relative humidity (up to 60%), good repeatability were achieved with the Cu-BTC/PANI nanocomposite film-grown QCM sensor.**

**†These authors equally contributed to this work.**

***Corresponding author e-mail: sskim@ucalgary.ca**

## I. INTRODUCTION

Hydrogen gas is emerging as a renewable and sustainable energy source and has been utilized in various applications such as fuel cells, weather balloons, cryogenic fuels and friction-heat removal in turbines. Hydrogen gas has also been commonly used in aerospace, biomedical systems and refineries [1]. However, when hydrogen gas concentration exceeds 4% in air, it is easily flammable and highly explosive [2]. Very low energy is required to ignite hydrogen-air mixtures [3], and thus sensitive and selective hydrogen sensors are required for safety purposes. Many current hydrogen sensors utilize inorganic metal oxides such as $SnO_2$, ZnO, $TiO_2$ and palladium alloys [4]. However, metal oxide films require high operating temperature and are partially selective to hydrogen. Palladium and zinc oxide are common materials used to detect hydrogen, but they are also sensitive to other gases such as oxygen and methane which limit their chemical selectivity to hydrogen [3], [5]. Therefore, conducting polymers and metal-organic frameworks (MOFs, also known as coordination polymers) have recently garnered significant attention to address operating temperature and chemical selectivity issues of palladium and metal oxides-based hydrogen sensors.

MOFs are one-, two- or three-dimensional crystalline structure materials that have been widely studied for gas sorption and storage. However, there have been limited reports on the utilization of MOFs for gas sensing. It is important to control the specific surface area of the MOFs film to maximize the gas sensing capabilities [6]. In our previous work, we have demonstrated the ability to control the MOFs' crystal size through varying the organic ligand concentrations or ultrasonic treatment time [7]. Due to the low adsorption enthalpy of physical adsorption, MOFs-based gas sensors can operate at room temperatures. Furthermore, the reactions are reversible and exhibit fast response time typically in the range of 10 s [8]. The adsorption capacity is significantly reduced at higher temperatures [6]. In this work, Cu-BTC, which has the micro-scale porosity and exceptionally high specific surface area arising from the cubic framework [9], is employed as a base sensing material. Ultrahigh porosity and specific surface area make Cu-BTC highly appealing for gas sensing applications.

Cu-BTC is a material that has been previously studied for hydrogen adsorption [9] and it showed high hydrogen uptake even at low pressures (< 0.6 MPa) due to the high heat of adsorption [6]. This makes Cu-BTC a good candidate for hydrogen sensing material. Cu-BTC has two predominant pore sizes at 0.5 nm and 0.9 nm due to the complex channel/pocket structure [10]. Furthermore, it has been suggested that these MOFs rely on the presence of unsaturated metal centers to allow physisorption and chemical interaction [11]. The high affinity of hydrogen with Cu-BTC results from the presence of open metal sites (Cu ion sites) [9]. Moreover, theoretical calculations on carbon structures suggest that hydrogen adsorption is preferred in small micropores [12]. This is the case for Cu-BTC, which has two types of pores: the main pores of 0.9 nm and smaller pores with windows of 0.5 nm diameter [13].

Polyaniline (PANI) is one of the most common conducting polymers used in sensors due to low fabrication costs, ease of deposition, capabilities of chemical structure modification, stability in air, and capability of room temperature operation [1], [2]. Changes in the electrical and mechanical properties of PANI emeraldine salt upon exposure to hydrogen gas make it

very appealing sensor material [3]. PANI has commonly been used for hydrogen sensing because conjugated π-bonds can be easily changed [14]. The electrical conductivity increases seen in PANI are also attributed to the production of more protons in the PANI backbone as hydrogen is adsorbed [15].

A quartz crystal microbalance (QCM) has recently emerged as a highly sensitive device for multimodal gas sensing and adsorption/desorption analysis. Lu et al. demonstrated the effectiveness of MOF-coated QCM for measuring ammonia vapour through adsorbed mass changes [16]. Detecting low concentrations of gas using only resonance frequency change of nanostructure-coated QCM is mostly challenging [17]. Therefore, present work exploits multimodality of QCM which provides simultaneous signals (resonance frequency and motional resistance). We found that motional resistance change exhibited faster response and recovery time over resonance frequency change with our nanostructure-coated QCM sensors.

In this work, Cu-BTC/PANI nanocomposite film is synthesized on a QCM by using intense pulsed light (IPL). The Cu-BTC/PANI composite film increases adsorption and improves selectivity compared to Cu-BTC film. IPL enables the formation of fibrous Cu-BTC/PANI composite film on a QCM in seconds. This dramatically reduces the day-long processing time and energy requirements for synthesis of MOFs using conventional solvothermal methods [18]. In addition, PANI significantly enhanced the selectivity of Cu-BTC to hydrogen against other gases such as $CH_4$ and $CO_2$.

## II. Materials and Methods

### A. Materials

Trimesic acid (1,3,5-benzene tricarboxylic acid ($H_3BTC$), 98%, Alfa Aesar), polyaniline emeraldine salt (Sigma Millipore), ammonium persulfate ($(NH_4)_2S_2O_8$, 98%, Aldrich), sodium hydroxide (NaOH, 99%, VWR), acetone ($(CH_3)_2CO$, 99%, VWR), and distilled deionized water (DDW) were used without further purification in the synthesis of Cu-BTC and Cu-BTC/PANI composite films. A quartz crystal, a thin disk of 1 inch diameter, AT-cut, α-quartz with circular electrodes patterned on both sides, was utilized as a resonator (Stanford Research Systems, Sunnyvale, CA, USA).

### B. Synthesis of Cu-BTC and Cu-BTC/PANI nanocomposite films on QCM sensors

A 200 nm thin Cu layer was sputter coated on an active area of quartz crystal using a stainless steel shadow mask with a 0.5-inch diameter hole. The Cu film was then oxidized using a strong oxidizing aqueous solution of 4 ml sodium hydroxide (NaOH, 10M), 2 ml ammonium persulfate ($(NH_4)_2S_2O_8$ , 1M) and 9 ml DDW. $Cu(OH)_2$ nanowires were formed after 30 min of oxidation. A precursor solution of 0.1 mM BTC and a 0.1 mM BTC solution mixed with 0.5 mg of PANI were used for the synthesis of Cu-BTC film and Cu-BTC/PANI composite film, respectively. After applying each precursor solution to the $Cu(OH)_2$ film on QCM, multiple IPL were exposed to the surfaces and resulted in fully converted Cu-BTC film and Cu-BTC/PANI composite film, respectively. Multiple IPL provided the sufficient energy required for the MOFs film synthesis [19]. The obtained films were washed by ethanol and DDW, then dried for 2 h at 70◦C under vacuum in order to remove any solvents stuck in the pores.

### C. Apparatus for characterizations of films

The changes in the resonance frequency and motional resistance of Cu-BTC or Cu-BTC/PANI film-grown quartz crystal sensor, caused by adsorbed hydrogen, were simultaneously measured by a QCM200 system (Stanford Research Systems, Sunnyvale, CA, USA).

The QCM200 uses a commercially available 5 MHz, 1 inch diameter, AT-cut quartz crystal with circular electrodes on both sides which is oscillated by a QCM25 crystal oscillator. The sensor chamber volume is approximately 0.15 mL. The morphologies of the Cu-BTC film and Cu-BTC/PANI composite film were characterized by a field emission scanning electron microscope (FE-SEM, Quanta$^{TM}$ 250). The crystalline structures were characterized by using an x-ray diffractometer (XRD, Rigaku Multiflex).

### D. Method for gas sensing

The flow chamber, shown in Figure 1, was first flooded with 1000 $cm^3$/min [20] nitrogen gas (99.998% purity, Praxair) for 10 minutes to remove contaminants from the film surface. The gas flow rate was maintained constant at 1000 $cm^3$/min throughout the experiments. The QCM 200 system was used to obtain both resonance frequency and motional resistance at ambient pressure and room temperature. The test gas was then fed in at controlled ratios with mass flow controllers (MFC, AtoVac GMC1200, Suwon, South Korea) with nitrogen as the carrier gas to achieve target concentations. A bubbler filled with DDW was utilized to control relative humidity (RH) and a humidity sensor (FisherScientific, USA) was used to measure RH. 4% hydrogen balanced with nitrogen gas, 99 % carbon dioxide, 4 % methane balanced with nitrogen gas were used as test gases. Various concentrations of hydrogen gas at different RH were tested to determine the selectivity and sensitivity of our sensors at ambient pressure and room temperature. An environmental sensor (SparkFun, USA) was used to measure temperatures and pressure.

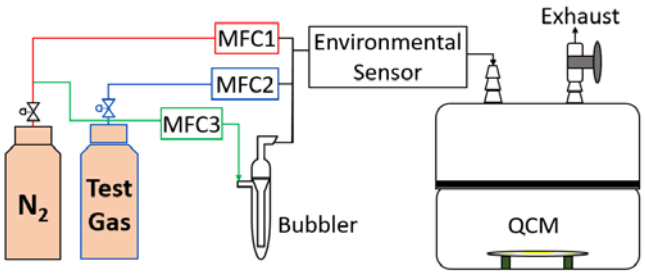


Fig. 1. A schematic representation for hydrogen sensing setup using a QCM 200 system.

## III. Results and Discussion

### A. Sensing film preparation and characterization

Cu-BTC thin films deposited on various substrates were previously reported by several methods including solvothermal [20], layer by layer [21], and seeded growth [16] to name a few. Among them, the direct growth approach has shown its feasibility in the rapid fabrication of uniform, dense, strongly

attached MOFs thin films on metal substrates [7], [19]. Here, we demonstrate a simple protocol for the rapid syntheses of Cu-BTC and Cu-BTC/PANI nanocomposite films under ambient conditions using IPL. Figure 2 shows a schematic representation for the fabrication of the sensing layer on a QCM by using the IPL method.

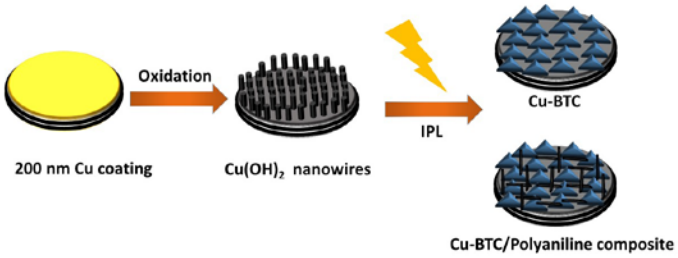


Fig. 2. Schematic illustration of the two-step method for the fabrication of sensing films (Cu-BTC or Cu-BTC/PANI nanocomposite).

Here, the Cu-based MOF film is directly synthesized on a copper film-coated QCM. Firstly, the metal substrate is oxidized to yield the metal hydroxide layer. This step is important because transformation from metal to metal hydroxide facilitates the liberation of metal ions, consequently metal ions will coordinate with organic ligands to form Cu-MOFs [22]. Coated copper film is treated with oxidizing solution for 30 min to form $Cu(OH)_2$ nanowires as shown in Figure 3. The advantages of using metal hydroxide compared to bare metal substrate are coming from less binding energy and larger surface area. The Cu ion in hydroxide has binding energy of 916.5 eV and Cu ion in metal has 932.61 eV [23]. Also, the high surface area of $Cu(OH)_2$ nanowires shown in Figure 3(b) facilitates more chemical reactions compared to smooth surface shown in Figure 3(a).

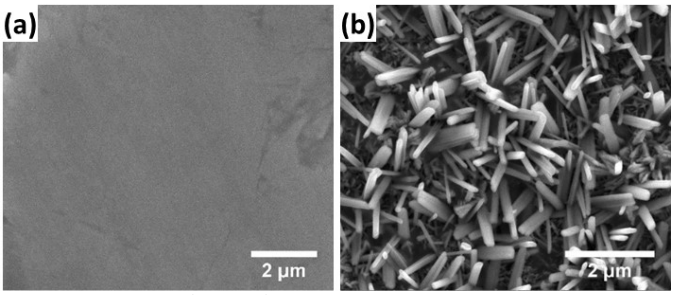


Fig. 3. SEM images of (a) Cu-film, (b) $Cu(OH)_2$ nanowires.

XRD is used to confirm the conversion from copper to the corresponding copper hydroxides. Figure 4 reveals that new peaks appear after oxidation of the copper film which represent conversion of pure copper film to copper hydroxide. Three new peaks at $2\theta$ = 16.9°, 24.02° and 34.28° appear after oxidation which correspond to (202), (021) and (002), respectively, for $Cu(OH)_2$ nanowires [24].

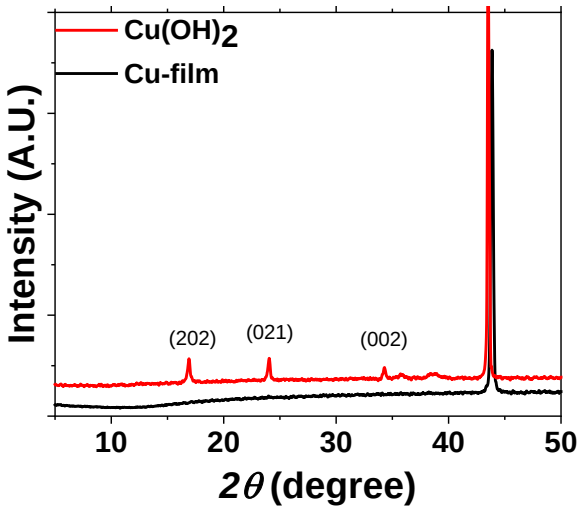


Fig. 4. XRD patterns of Cu-film (black) and $Cu(OH)_2$ nanowires on Cu-film (red).

Cu-BTC film and Cu-BTC/PANI nanocomposite film can be simply formed by drop and dry the corresponding organic ligand solution on copper hydroxide nanowire-grown quartz crystal then subject to multiple IPL at ambient conditions. The films can be developed in less than 3 min with good homogeneity and crystallinity. The Cu-BTC film is grown after 15 pulses of IPL according to our previous work [19]. The IPL technique greatly facilitates the growth of dense MOF films with good homogeneity and crystallinity.

The crystallinity of the synthesized Cu-BTC and Cu-BTC/PANI film is characterized by using XRD as shown in Figure 5. The XRD patterns unequivocally reveal the presence of Cu-BTC diffraction peaks in both films. The grown Cu-BTC layer shows a significant preferred orientation along the (222) crystallographic direction. This result matches well with our previous work [7]. We notice that the intensity of Cu-BTC peaks decreases when Cu-BTC/PANI nanocomposite is synthesized. This may be due to the formation of nanocomposite that may lower the degree of Cu-BTC crystallinity. As shown in Figure 5, the very small peak corresponds to PANI appear in the region between $2\theta$ = 25-30° which matches with previous reports [25], [26].

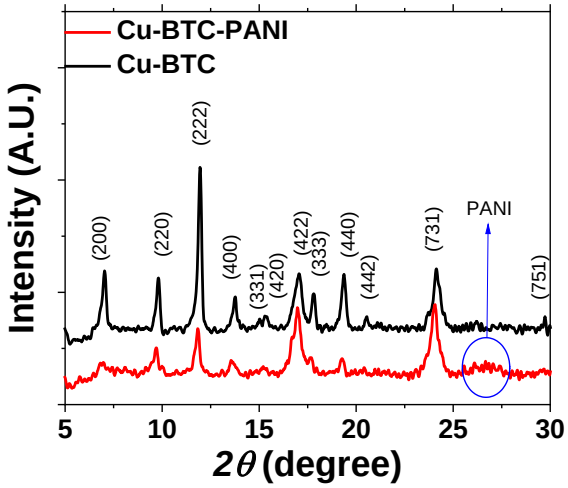


Fig. 5. XRD patterns of Cu-BTC film (black) and Cu-BTC/PANI nanocomposite film (red).

The morphology of the prepared films is investigated by SEM. The SEM images of both Cu-BTC and Cu-BTC/PANI nanocomposite are shown in Figure 6. The surfaces of all the obtained films are continuously uniform without visible cracks and defects, which are very desirable for gas sensing applications. Interestingly, Cu-BTC/PANI nanocomposite forms a fibrous shape as visible in Figure 6(c). The IPL here may play combined role for developing the Cu-BTC embedded on the PANI nanofibres. The enhanced generation of PANI nanofibers is attributed to IPL which has an adjustable energy range from 3 to 27 J for a 6 ms pulse. The IPL results in rapid localized temperature spikes that result in the formation of fibrous structures [27]. The interaction with photons makes the aniline monomer excited and helps the formation of aniline radical cations and oligomeric intermediates, leading the formation of PANI nanofibers [28]. As shown in Figure 6(d) at higher magnification, Cu-BTC nanocrystals seem to be densly embedded on several micron-long PANI nanofibres. This makes very rough surfaces on Cu-BTC/PANI nanocomposite fibres.

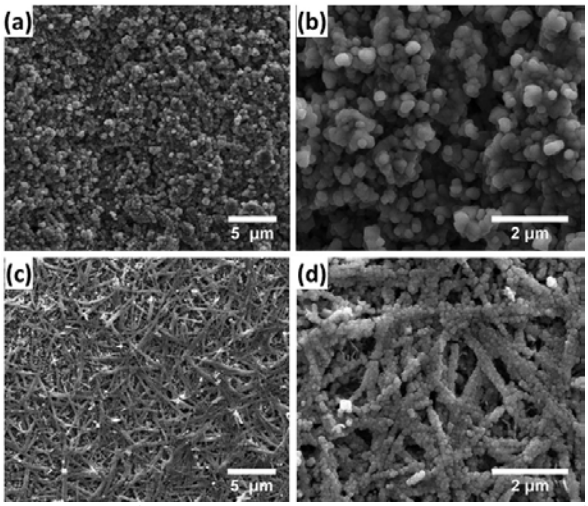


Fig. 6. SEM images of (a,b) Cu-BTC, and (c,d) Cu-BTC/PANI composite films grown on quartz crystals at lower and higher magnification, respectively.

The addition of PANI caused the thickness of the film to increase from approximately 638 nm (Cu-BTC) to 916 nm (Cu-BTC/PANI). This can be seen from cross-sectional SEM images shown in supporting information Figure S1. Usually, the film thickness more than ~ 1 µm is not recommended for QCM sensing applications because a thicker sensing layer may cause the signal of a QCM to become unstable [29]. Our sensing films are less than 1 µm thick and show very stable signals for gas sensing experiments in the following section.

The SEM images together with the XRD patterns demonstrate that our direct growth method is a very promising technique for the simple fabrication of MOF composite films on QCM sensors.

### *B. Hydrogen sensing responses*

The sensing chamber is first flooded with 1000 $cm^3$/min of nitrogen gas for 10 minutes to reach ambient steady-state conditions ($R_0$, $f_0$). Longer durations are tested, but the effect is negligible. Target gases are then mixed into the input stream at controlled concentrations with MFCs. Initially, the gases are allowed to run until a peak value ($R_g$, $f_g$) is reached. The adsorption and swelling within the sensing material give rise to changes in resonsnace frequency and motional resistance of QCM sensors [30]. A response similar to Xia et al. for hydrogen sensing with $TiO_2$ is noted [31]. A sharp decrease in the frequency is followed by a modest increase before settling at an equilibrium rate (see supporting information Figure S2). Therefore, hydrogen gas is only run until the first peak is reached. It is found that 5 seconds is sufficient for the initial peak response to be reached. When the hydrogen gas is turned off and only nitrogen gas is fed into the flow cell, it is found that up to 25 seconds is required to reach ambient steady-state conditions. The hydrogen sensing response curves of the developed sensors are demonstrated in Figure 7(a)-(d). The initial frequency, $f_0$, and motional resistance, $R_0$, for the Cu-BTC/PANI film-grown QCM are 4,989,710 Hz and 0.862 kΩ, respectively, and those of the Cu-BTC film-grown QCM are 4,995,012 Hz and 0.978 kΩ, respectively. The changes in the resonance frequency and motional resistance of the QCM are simultaneously measure at hydrogen concentrations ranging from 40 ppm to 800 ppm. The results show that both the Cu-BTC and Cu-BTC/PANI film-grown QCM sensors show noticeable changes to 40 ppm hydrogen at room temperature and ambient pressure. Testing up to 800 ppm is done to provide sufficient data points for data fitting to determine the limit of detection (LOD) of each sensor.

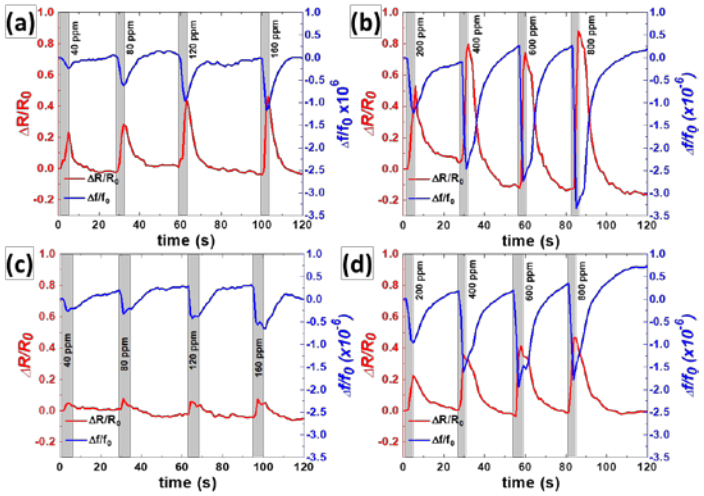


Fig. 7. Resonance frequency (blue) and motional resistance (red) change response curves for (a) Cu-BTC/PANI at low $H_2$ gas concentrations; (b) Cu-BTC/PANI at high $H_2$ gas concentrations; (c) Cu-BTC at low $H_2$ gas concentrations; (d) Cu-BTC at high $H_2$ gas concentrations.

A good indicator of the condition of the mass sensing crystal is the motional resistance $R$ in the equivalent circuit of a quartz crystal resonator. This motional resistance increases as more material are adsorbed onto the quartz crystal and more energy dissipated. This is due to the increase of acoustic losses in the deposited material [29]. The changes in motional resistance are used to compare the sensitivities of two sensors. The primary sensor response is defined as $\Delta R/R_0$ which is the initial motional resistance subtracted from the peak resistance caused by $H_2$ adsorption divided by the initial resistance. At the low concentrations (40-160 ppm), it was found that the sensor response of Cu-BTC/PANI film-grown QCM is 5.2 times larger

than regular Cu-BTC film-grown QCM. By comparison, at high concentrations, the sensor response of Cu-BTC/PANI film-grown QCM is still approximately 2.0 times larger than regular Cu-BTC film-grown QCM. The improved performance can be attributed to an increase in the affinity and active sensing surface area of Cu-BTC/PANI nanocomposite film to hydrogen.

The response of the Cu-BTC/PANI film-grown QCM sensor approximately follows a logarithmic model shown in equation (1) where $C_{H2}$ is hydrogen concentration in ppm.

$$\left(\frac{\Delta R}{R_0}\right)_{Cu-BTC/PANI} = 0.1948 \ln\left(C_{H_2}\right) - 0.4493 \quad (1)$$

This fit has an $R^2$ of 0.96. The largest noise signal measured corresponds to 0.0271. Thus, the LOD should occur when the response is 0.0814 to achieve a signal-to-noise of 3. Using equation (1), the LOD for the Cu-BTC/PANI film-grown QCM sensor is determined to be 15 ppm. By comparison, the LOD for Cu-BTC film-grown QCM sensor is determined to be approximately 88 ppm. A logarithmic gas sensor response has also been noted in other work [32], but the exact physics of the response requires further investigation.

### *C. Selectivity, reproducibility, and stability of Cu–BTC and Cu-BTC/PANI film-grown QCM sensors*

Even though Cu-BTC film-grown QCM sensor show good response to hydrogen, it was reported that Cu-BTC responded more to $CO_2$ (~90:1 $CO_2$:$H_2$) and $CH_4$ (~15:1 $CH_4$:$H_2$) [10]. Figure 8 clearly shows resonance frequency and motional resistance changes of Cu-BTC film-grown QCM (blue) due to $CO_2$ and $CH_4$ adsorption. However, Cu-BTC/PANI nanocomposite film-grown QCM sensor demonstrates negligible resonance frequency and motional resistance changes due to reduced adsorption of larger molecules such as $CO_2$ and $CH_4$ as shown in Figure 8. In particular, PANI exhibits low permeability to $CH_4$ versus $CO_2$ [33]. This is attributed to almost no sensing responses for $CH_4$ in Figure 8(b) and 8(d) with a Cu-BTC/PANI film-grown QCM sensor. There is no trend that can be observed in the responses after injection of $CH_4$ or $CO_2$. PANI is introduced in the organic solvent functionalization to enhance the Cu-BTC's selectivity for hydrogen. $H_2$ gas may form a bridge between nitrogen atoms on the two adjacent chains of PANI or there may be partial protonation of some of the nitrogens in imine group [1]. The incorporation of PANI with Cu-BTC helps attain better selectivity and sensitivity for hydrogen gas over methane and carbon dioxide.We speculate that high PANI surface concentration minimize the penetration of $CH_4$ and $CO_2$ to the Cu-BTC resulting in high selectivity to $H_2$.

Figure 9 (a) and (b) show the magnitude of changes in motional resistance and resonance frequency becomes approximately a half when 20% RH is introduced. Cu-BTC has previously been reported to adsorb water molecules and show sensitivity to humidity [34]. PANI has also been shown as sensitive to humidity [35]. However, we speculate that the addition of PANI limits the adsorption of water molecules into the Cu-BTC. Therefore, even though a decrease in the sensor response is observed, Cu-BTC/PANI composite film-grown QCM sensor still responds to hydrogen. The response time of the sensors, at all humidity levels, remained almost constant at around 3 seconds. The recovery times varied from 3 s for 200 ppm to 20 s for 800 ppm.

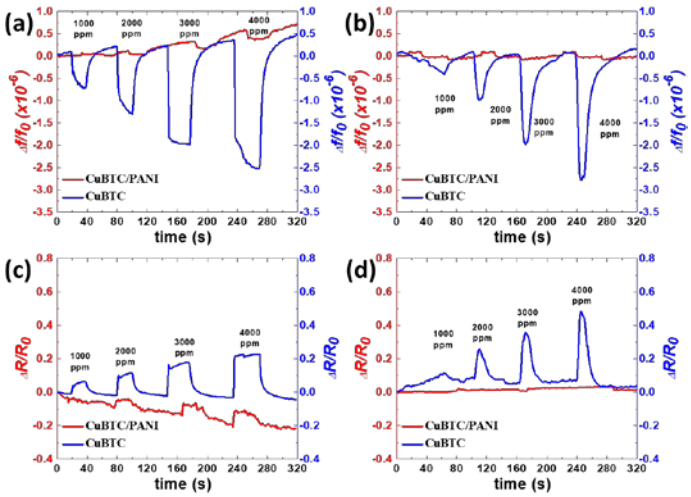


Fig. 8. Frequency change upon injecting (a) $CO_2$ and (b) $CH_4$ and motional resistance change upon injecting (c) $CO_2$ and (d) $CH_4$ for both Cu-BTC film-grown QCM (blue) and Cu-BTC/PANI film-grown QCM (red), respectively.

The sensor responses steadily decrease as the relative humidity increases as shown in Figure 9 (c). In regular Cu-BTC samples, the adsorbed water molecules often displace BTC ligands and ultimately degrade the Cu-BTC [36]. Furthermore, it has been suggested that the hydrogen sensing properties of PANI are completely suppressed by the presence of humidity [3]. The responses between Cu-BTC/PANI composite at 20% RH ($\Delta R/R_0$ = 0.473 for 800 ppm and 0.230 for 200 ppm) and Cu-BTC at 0% RH (0.486 for 800 ppm and 0.227 for 200 ppm) becomes comparable. This may suggest that the water molecules have higher affinity to PANI than to Cu-BTC, so that the water has less effect on the Cu-BTC. The reduction in the response can be attributed to the suppressed hydrogen sensing by PANI resulting from preferential interaction with water molecule over hydrogen [3]. The relations between motional resistance response and $H_2$ concentration are shown in supporting information section S3 for each relative humidity.

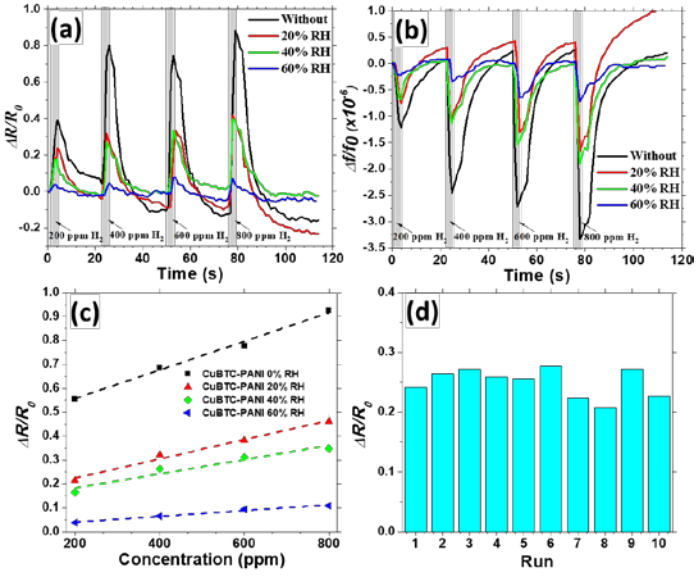

Fig. 9. Hydrogen sensing response curves of Cu-BTC/PANI composite film at varying humidity levels measured as (a) normalized motional resistance change, (b) normalized resonance frequency change. The normalized motional resistance changes of a Cu-BTC/PANI film-growm QCM as a function of hydrogen concentration at varying humidity levels are plotted in (c). Repeatability test for Cu-BTC/PANI film-grown QCM sensing of 40 ppm hydrogen in dry nitrogen is shown in (d).

Inherent sensor variation from sample to sample inevitably arises during the fabrication processes of sputter coating, solution-based oxidation, materials synthesis with IPL. Therefore, 10 sensors are fabricated and tested repeatedly at 40 ppm as shown in Figure 9(d). 40 ppm of hydrogen is the current limit of our testing apparatus. The Cu-BTC/PANI film-grown QCM sensors show an average response ($\Delta R/R_0$) of 0.250 ± 0.023 at 40 ppm. The results of each run are shown in Figure 9(d). The sensor that achieved nearest to the average response sensitivity, recovery and response time are used to report the data above.

The sensor baseline experiences a small amount of drift. In general, the drift appears to decrease as the humidity increases. Such changes are generally attributed to thermal drift due to changes in the ambient conditions [37]. In this study, adjustments are not made for small ambient changes in temperature, pressure, and minor fluctuations in the injection flow rate from the MFCs.

## IV. Conclusion

In conclusion, Cu-BTC and Cu-BTC/PANI composite film-grown QCMs are successfully fabricated using IPL. The Cu-BTC/PANI composite film-grown QCM shows significantly improved hydrogen sensing performance versus the regular Cu-BTC film-grown QCM. The in-situ growth of PANI on Cu-BTC ensures the interaction of the Cu-BTC and PANI. The combination of Cu-BTC/PANI produces gas sensors that are more selective to hydrogen. In addition, a fast response time of 3 s and good selectivity versus $CH_4$ and $CO_2$ are noted for the composite film. The motional resistance responses exhibit a near linear behaviour between 200 ppm and 800 ppm, but the overall responses taking into account lower concentrations best fit a logarithmic model. This model estimates the LOD to be 15 ppm for a Cu-BTC/PANI composite film-grown QCM sensor. Furthermore, we are able to overcome humidity poisoning effects that commonly plague hydrogen sensors consisting of solely Cu-BTC or PANI. The combination of PANI with Cu-BTC produces gas sensors that are more selective to hydrogen.

## V. Acknowledgements

The authors are very grateful for the support from the Natural Sciences and Engineering Research Council of Canada (NSERC) Discovery Grant Program. O. Abuzalat would like also to acknowledge Military Technical College, Egyptian Armed Force for their financial support.

## VI. References

[1] R. Arsat, X. F. Yu, Y. X. Li, W. Wlodarski, and K. Kalantar-zadeh, “Hydrogen gas sensor based on highly ordered polyaniline nanofibers,” *Sensors Actuators B Chem.*, vol. 137, no. 2, pp. 529–532, Apr. 2009.

[2] S. Srivastava, S. S. Sharma, S. Agrawal, S. Kumar, M. Singh, and Y. K. Vijay, “Study of chemiresistor type CNT doped polyaniline gas sensor,” *Synth. Met.*, vol. 160, no. 5–6, pp. 529–534, Mar. 2010.

[3] S. Virji, R. B. Kaner, and B. H. Weiller, “Hydrogen Sensors Based on Conductivity Changes in Polyaniline Nanofibers,” *J. Phys. Chem. B*, vol. 110, pp. 22266–22270, 2006.

[4] C. Wang, L. Yin, L. Zhang, D. Xiang, and R. Gao, “Metal Oxide Gas Sensors: Sensitivity and Influencing Factors,” *Sensors*, vol. 10, no. 3, pp. 2088–2106, Mar. 2010.

[5] Syed Mubeen, Ting Zhang, Bongyoung Yoo, * and Marc A. Deshusses, and N. V. Myung*, “Palladium Nanoparticles Decorated Single-Walled Carbon Nanotube Hydrogen Sensor,” 2007.

[6] M. Hirscher, B. Panella, and B. Schmitz, “Metal-organic frameworks for hydrogen storage,” *Microporous Mesoporous Mater.*, vol. 129, no. 3, pp. 335–339, Apr. 2010.

[7] O. Abuzalat, D. Wong, M. Elsayed, S. Park, and S. Kim, “Sonochemical Fabrication of Cu(II) and Zn(II) Metal-Organic Framework Films on Metal Substrates,” *Ultrason. Sonochem.*, Mar. 2018.

[8] A. Lan *et al.*, “A Luminescent Microporous Metal–Organic Framework for the Fast and Reversible Detection of High Explosives,” *Angew. Chemie Int. Ed.*, vol. 48, no. 13, pp. 2334–2338, Mar. 2009.

[9] B. Panella, M. Hirscher, H. Pütter, and U. Müller, “Hydrogen Adsorption in Metal–Organic Frameworks: Cu-MOFs and Zn-MOFs Compared,” *Adv. Funct. Mater.*, vol. 16, no. 4, pp. 520–524, Mar. 2006.

[10] Q. Yang and C. Zhong, “Molecular Simulation of Carbon Dioxide/Methane/Hydrogen Mixture Adsorption in Metal-Organic Frameworks,” *J. Phys. Chem. B*, vol. 110, pp. 17776–17783, 2006.

[11] J. R. Karra and K. S. Walton, “Effect of Open Metal Sites on Adsorption of Polar and Nonpolar Molecules in Metal−Organic Framework Cu-BTC,” *Langmuir*, vol. 24, no. 16, pp. 8620–8626, Aug. 2008.

[12] Q. Wang and J. K. Johnson, “Molecular simulation of hydrogen adsorption in single-walled carbon nanotubes and idealized carbon slit pores,” *J. Chem. Phys.*, vol. 110, no. 1, p. 577, Dec. 1998.

[13] Aleksey Vishnyakov, Peter I. Ravikovitch, Alexander V. Neimark, Martin Bülow, and Q. M. Wang§, “Nanopore Structure and Sorption Properties of Cu−BTC Metal−Organic Framework,” *Nano Lett.*, vol. 3, no. 6, pp. 713–718, 2003.

[14] L. Al-Mashat *et al.*, “Graphene/Polyaniline Nanocomposite for Hydrogen Sensing,” *J. Phys. Chem. C*, vol. 114, pp. 16168–16173, 2010.

[15] C. O. Baker, X. Huang, W. Nelson, and R. B. Kaner, “Polyaniline nanofibers: broadening applications for conducting polymers,” *Chem. Soc. Rev.*, vol. 46, no. 5, pp. 1510–1525, Mar. 2017.

[16] G. Lu *et al.*, “Fabrication of Metal-Organic Framework-Containing Silica-Colloidal Crystals for Vapor Sensing,” *Adv. Mater.*, vol. 23, no. 38, pp.

4449–4452, Oct. 2011.
[17] A. Phani, V. Putkaradze, J. E. Hawk, K. Prashanthi, and T. Thundat, “A nanostructured surface increases friction exponentially at the solid-gas interface,” *Sci. Rep.*, vol. 6, no. 1, p. 32996, Dec. 2016.
[18] F. Song, Q. Zhong, and Y. Zhao, “A protophilic solvent-assisted solvothermal approach to Cu-BTC for enhanced CO $_2$ capture,” *Appl. Organomet. Chem.*, vol. 29, no. 9, pp. 612–617, Sep. 2015.
[19] C. Yim, O. Abuzalat, M. Elsayed, S. Park, and S. Kim, “Rapid Fabrication of Metal–Organic Framework Films from Metal Substrates Using Intense Pulsed Light,” *Cryst. Growth Des.*, vol. 18, no. 11, pp. 6946–6955, Nov. 2018.
[20] P. Davydovskaya, A. Ranft, B. V. Lotsch, and R. Pohle, “Analyte Detection with Cu-BTC Metal–Organic Framework Thin Films by Means of Mass-Sensitive and Work-Function-Based Readout,” *Anal. Chem.*, vol. 86, no. 14, pp. 6948–6958, Jul. 2014.
[21] O. Shekhah, “Layer-by-Layer Method for the Synthesis and Growth of Surface Mounted Metal-Organic Frameworks (SURMOFs),” *Materials (Basel).*, vol. 3, no. 2, pp. 1302–1315, Feb. 2010.
[22] K. Okada *et al.*, “Copper Conversion into Cu(OH) $_2$ Nanotubes for Positioning Cu $_3$ (BTC) $_2$ MOF Crystals: Controlling the Growth on Flat Plates, 3D Architectures, and as Patterns,” *Adv. Funct. Mater.*, vol. 24, no. 14, pp. 1969–1977, Apr. 2014.
[23] M. C. Biesinger, L. W. M. Lau, A. R. Gerson, and R. S. C. Smart, “Resolving surface chemical states in XPS analysis of first row transition metals, oxides and hydroxides: Sc, Ti, V, Cu and Zn,” *Appl. Surf. Sci.*, vol. 257, no. 3, pp. 887–898, Nov. 2010.
[24] D. Bradshaw, A. Garai, and J. Huo, “Metal–organic framework growth at functional interfaces: thin films and composites for diverse applications,” *Chem. Soc. Rev.*, vol. 41, no. 6, pp. 2344–2381, Feb. 2012.
[25] S. Wannapaiboon, M. Tu, and R. A. Fischer, “Liquid Phase Heteroepitaxial Growth of Moisture-Tolerant MOF-5 Isotype Thin Films and Assessment of the Sorption Properties by Quartz Crystal Microbalance,” *Adv. Funct. Mater.*, vol. 24, no. 18, pp. 2696–2705, May 2014.
[26] K. Vadiraj and S. Belagali, “Characterization of Polyaniline for Optical and Electrical Properties,” *IOSR J. Appl. Chem. (IOSR-JAC*, vol. 8, no. 1, pp. 53–56, 2015.
[27] T. Druffel, R. Dharmadasa, B. W. Lavery, and K. Ankireddy, “Intense pulsed light processing for photovoltaic manufacturing,” *Sol. Energy Mater. Sol. Cells*, vol. 174, pp. 359–369, Jan. 2018.
[28] Y. Wang, “Preparation and application of polyaniline nanofibers: an overview,” *Polym. Int.*, vol. 67, no. 6, pp. 650–669, Jun. 2018.
[29] C. Lu and A. W. Czanderna, *Applications of Piezoelectric Quartz Crystal Microbalances*. Elsevier Science, 1984.
[30] S. C. Howard, V. S. J. Craig, P. A. Fitzgerald, and E. J. Wanless, “Swelling and Collapse of an Adsorbed pH-Responsive Film-Forming Microgel Measured by Optical Reflectometry and QCM,” *Langmuir*, vol. 26, no. 18, pp. 14615–14623, 2010.
[31] X. Xia, W. Wu, Z. Wang, Y. Bao, Z. Huang, and Y. Gao, “A hydrogen sensor based on orientation aligned TiO2 thin films with low concentration detecting limit and short response time,” *Sensors Actuators B Chem.*, vol. 234, pp. 192–200, Oct. 2016.
[32] A. Teeramongkonrasmee and M. Sriyudthsak, “Methanol and ammonia sensing characteristics of sol–gel derived thin film gas sensor,” *Sensors Actuators B Chem.*, vol. 66, no. 1–3, pp. 256–259, Jul. 2000.
[33] N. V. Blinova and F. Svec, “Functionalized polyaniline-based composite membranes with vastly improved performance for separation of carbon dioxide from methane,” *J. Memb. Sci.*, vol. 423–424, pp. 514–521, Dec. 2012.
[34] P. Davydovskaya, R. Pohle, A. Tawil, and M. Fleischer, “Work function based gas sensing with Cu-BTC metal-organic framework for selective aldehyde detection,” *Sensors Actuators B Chem.*, vol. 187, pp. 142–146, Oct. 2013.
[35] S. Kotresh, Y. T. Ravikiran, H. G. Raj Prakash, C. V. V. Ramana, S. C. Vijayakumari, and S. Thomas, “Humidity sensing performance of spin coated polyaniline–carboxymethyl cellulose composite at room temperature,” *Cellulose*, vol. 23, no. 5, pp. 3177–3186, Oct. 2016.
[36] N. Al-Janabi *et al.*, “Mapping the Cu-BTC metal–organic framework (HKUST-1) stability envelope in the presence of water vapour for CO2 adsorption from flue gases,” *Chem. Eng. J.*, vol. 281, pp. 669–677, Dec. 2015.
[37] A. Rivadeneyra, J. Fernández-Salmerón, M. Agudo, J. A. López-Villanueva, L. F. Capitan-Vallvey, and A. J. Palma, “Design and characterization of a low thermal drift capacitive humidity sensor by inkjet-printing,” *Sensors Actuators B Chem.*, vol. 195, pp. 123–131, May 2014.

**Osama Abuzalat** is a Ph.D. candidate at the Department of Mechanical and Manufacturing Engineering, University of Calgary.

**Danny Wong** is a Ph.D. student at the Department of Mechanical and Manufacturing Engineering, University of Calgary.

**Simon S. Park** is a Professor at the Department of Mechanical and Manufacturing Engineering, University of Calgary.

**Seonghwan Kim** is an Associate Professor and Canada Research Chair in Nano Sensing Systems at the Department of Mechanical and Manufacturing Engineering, University of Calgary.